

RAL 85108  
COPY 1 R61  
RAL-85-108

Science and Engineering Research Council  
**Rutherford Appleton Laboratory**  
CHILTON, DIDCOT, OXON, OX11 0QX

RAL-85-108

\*\*\*\*\* RAL LIBRARY R61 \*\*\*\*\*  
Acc\_No: 146111  
Shelf: RAL 85108  
E61  
Copy: 1

# A Report on the Mapping of the Didsy Sensor Responses as a Function of Micro-Meteorite Impact Position on the Giotto Bumper Shield

RADI, SPAC

A. Ridgeley

LIBRARY  
RUTHERFORD  
23 DEC 1985  
LABORATORY

December 1985

© Science and Engineering  
Research Council 1985

The Science and Engineering Research Council does not accept any responsibility for loss or damage arising from the use of information contained in any of its reports or in any communication about its tests or investigations.

A REPORT ON THE MAPPING OF THE DIDSY SENSOR RESPONSES AS A FUNCTION OF  
MICRO-METEORITE IMPACT POSITION ON THE GIOTTO BUMPER SHIELD

A Ridgeley

ABSTRACT

A realistic mock-up of the GIOTTO bumper shield has been used to calibrate the response of the flight bumper shield to micro-meteorite bombardment. A pulsed laser was used to simulate particle impacts, and a detailed mapping of the shield was made in order to determine the response of the DID sensors in terms of azimuthal and radial impact position.

1. INTRODUCTION

1.1 This report describes a calibration programme of work carried out in order to determine the response of the GIOTTO bumper shield to micro-meteorite particle impacts.

The GIOTTO spacecraft is scheduled to encounter Halley's comet during March 1986 at a relative velocity of  $68 \text{ km sec}^{-1}$ . At this encounter velocity quite small dust particles will mortally damage the spacecraft, which is therefore protected from dust particle impacts using a dual shield protection system. This comprises a 1mm thick aluminium alloy front shield and a 25mm thick kevlar and plastic foam rear shield mounted 250mm behind the front shield. Particles large enough to penetrate the front shields will generate a diverging cloud of debris which will impact the rear shield over a large area with much reduced penetrating ability.

The construction of the front part of the spacecraft showing the protective shield configuration is shown in fig 1.

1.2 The Dust Impact Detection System (DIDSY) experiment makes use of the impacts on the protection shields in order to measure the number and mass distribution of the impacting dust particles<sup>(1)(2)</sup>. The DIDSY experiment is divided into four sub-experiments.

- (i) The MSM sensors are three piezo-electric sensors mounted on the bumper shield to measure masses in the range  $10^{-10}$  -  $10^{-6}$  g.
- (ii) The RSM sensor is mounted on the rear shield to measure masses greater than  $10^{-6}$  g which can penetrate the bumper shield.
- (iii) The IPM is an impact measuring experiment mounted in a small plate mounted off the bumper shield. The bumper shield has a cut out to accommodate this experiment.
- (iv) The CIS is a capacitor bonded onto the top surface of the bumper shield.

The calibration work described in this report is in support of the MSM part of the experiment.

The aims of the DIDSY experiment have been taken into account in the design of the front shield, and design studies at RAL (using a pulsed laser to simulate particle impacts) have helped to produce the optimum design compatible with maintaining the structural integrity of the shield<sup>(3)</sup>. This design incorporates a clean and isolated 35° sector where better mass measurements can be made.

1.3 The aim of the DIDSY experiment is to determine the number (N) of dust particles of any given mass (m) at any given time (t) during the encounter with the comet. Clearly N is a function of m and r expressed

$$N = f(m) f(t)$$

f(t) is determined by the trajectory of the probe through the coma and f(m) describes the mass distribution of particles at a given point in the coma. The response of the MSM sensors on the bumper shield to any given impact depends not only on the mass of the particle but also on the position where the shield was impacted. The measured number of impacts at any given sensor response is therefore given by the convolution function

$$N_{\text{meas}} = N f(r, \theta)$$

where r and  $\theta$  are the radial coordinates of the shield.

In order to obtain the real mass distribution from the measured distribution the shield response has to be deconvoluted out, which means that f(r,  $\theta$ ) has to be determined.

Because the bumper shield has a complicated shape the response function can also be expected to be complicated so a determination of this function involves making a fairly detailed mapping of the bumper shield. Ideally this mapping would be carried out on the flight shield using a suitable stimulating technique. Because the shield is an integral part of the spacecraft structure, it is

impractical to consider such a calibration of the flight shield within the timescale available for the spacecraft preparation. The main calibration procedure has therefore had to be accomplished in isolation from the spacecraft, albeit with a limited amount of testing on the flight shield.

To this end two realistic mock-ups of the front shield have been built: one is located at the University of Kent at Canterbury, the other at RAL. Complementary calibration programmes have been conducted on these shields.

In addition there is a structural model (SM) spacecraft which has been constructed with a shield which is expected to be a very good copy of the flight model (FM) shield. The SM shield has not been available for a detailed mapping of its response but it has been available for a more extended calibration programme than has been possible with the FM shield. These measurements<sup>(4)</sup> have provided a valuable check on the validity of the mock-up shield measurements reported in this work.

## 2. THE RAL MOCK-UP SHIELD

2.1 The construction of the mock-up bumper shield is shown in Figure 2. It was intended that this shield would faithfully resemble the FM shield. The shield approximates to an annulus with inner radius 480mm and outer radius 929mm. There is a clean sector 35° wide isolated from the rest of the shield through two joints which are 99% acoustically isolating. The construction of these joints is described in ref (4). One of the piezo-electric sensors, designated DID4, is mounted on this clean sector 40mm from the inside edge and on the centre line of the sector.

The other two sensors, designated DID2 and DID3 are situated 50mm from the isolating joints on the large sector, and 227mm from the inside edge.

The large sector has various complicating parameters to its

structure imposed by space-craft considerations:

- (i) the sector is made in two pieces riveted together at an acoustically conducting joint. Details of this joint are also described in ref (4).
- (ii) There are various holes in the shield to accommodate four spring separation pads and two umbilical connection ports.
- (iii) There is a further hole where the impact plasma sensor (IPM) is situated.
- (iv) The capacitative impact sensor (CIS) is bonded onto this sector.
- (v) An additional piece (designated "the ear") has been riveted on. The ear protects the particle impact analyser experiment.
- (vi) An outer stiffening ring at radius 870 mm is riveted and bonded onto the underside of the shield for strengthening purposes. At the isolating joints this stiffening ring is broken and re-joined with joints containing viton rubber for damping. Details are again given in ref (4). This prevents acoustic waves being transmitted via the stiffening ring.
- (vii) There is an S-band antenna mounted on the shield.
- (viii) There is an inner stiffening ring attached to the shield through supporting pillars. One of these is attached to the small sector.

2.2 In all respects as described above the mock-up shield is near as possible an exact copy of the FM shield. There is an inadvertent deviation in one detail. The rivets joining the outer stiffening ring have been displaced one degree relative to the FM shield. Away from the front shield the mock-up does not try to exactly imitate the FM shield. The rear shield is represented by hollow ply-wood but joined to the front shield by means of realistic copies of the

FM support pillars. The kick motor which is situated in the hole in the middle of the FM shield is represented by a metal shell of similar shape. Again the interfaces with the front shield are realistic copies.

The most difficult problem encountered in simulating the FM shield was encountered with respect to the special conductive white paint with which the back of the FM shield is painted. This white paint was not available for coating the mock-up shields so any damping properties of this paint could not be properly simulated on the mock-ups.

A 250mm square piece of aluminium coated with the flight paint was made available for test purposes. From this sample an estimation of the damping properties was made by measuring the decay period following a stimulation. A search was then made for a material which caused a similar sized aluminium plate to decay with the same time constant.

It was found that Fablon CON-TACT satisfied this criterion. CON-TACT and the FM white paint coated samples decayed with a time constant of 2ms per order of magnitude decay compared with 10ms per order of magnitude decay for uncoated aluminium. The RAL mock-up shield was coated with CON-TACT in the hope of simulating the damping effect of the white paint on the FM shield except under the ear. This area was coated with the same conductive black paint used on the FM model.

The mock-up shield at Canterbury was left uncoated. The Canterbury mock-up shield should therefore compare with the SM shield which was also uncoated.

### 3. STIMULATION TECHNIQUES

- 3.1 It has been demonstrated by McDonnell<sup>(5)</sup> that particle impacts on sheet material generate a flexural wave motion which, in the DIDSY experiment, is detected by the piezo-electric sensors.

For particles speeds of greater than about  $10 \text{ km sec}^{-1}$  it is believed that there is a momentum enhancement due to crater formation<sup>(6)</sup>. At  $68 \text{ km sec}^{-1}$  the momentum enhancement is currently expected to be  $E = 12 \pm 3$ <sup>(7)</sup> based on experimental data from the 2MV Canterbury microparticle accelerator which extends, at present, to velocities of  $10 \text{ km sec}^{-1}$ . Because of this momentum enhancement, which has not been comprehensively studied experimentally, the ideal stimulation techniques for DIDSY calibration studies would be particles of  $10^{-10} \text{ g} - 10^{-6} \text{ g}$  mass range at a velocity of  $68 \text{ km/sec}$ . Such a stimulation technique is impracticable within existing technology and for practical purposes a choice has to be made of the following techniques all which have been investigated for DIDSY calibration purposes.

#### 3.1.1 Bead Drops

Glass or steel balls of a few mg mass are dropped from a height of about 100-200 mm. These particles have the same momentum as cometary dust particles in the  $10^{-8} - 10^{-7} \text{ g}$  mass range. The impact time is long with an inefficient conversion to high frequency flexural wave. Also the impact point is difficult to predict accurately and reproducibility of signal has been found to be poor.

#### 3.1.2 Piezo-Electric Stimulation

An electrical pulse is applied through a piezo-electric crystal to impart an impulse onto the target. This method has the advantage of having a short pulse time ( $\sim 1 \mu\text{s}$ ). The efficiency of electrical conversion is low however, so that signals are fairly low.

#### 3.1.3 Light Gas Gun (BMC)

In this method compressed nitrogen gas is used to project a particle of between  $100 \mu\text{g}$  and  $4 \text{ mg}$  mass at a velocity of about  $100 \text{ m sec}^{-1}$ . This method has proved to be a powerful stimulating technique and was used extensively in testing the SM shield and the FM shield.

The dispersion in the device makes the prediction of the impact point somewhat inaccurate (about 5mm diam circle). Reproducibility of signal is about +50%.

#### 3.1.4 Laser Pulses

The use of laser pulses to simulate particle impacts was proposed by Burton<sup>(8)</sup>, and the feasibility of using pulsed laser radiation to stimulate flexural wave motion was demonstrated by Reading and Ridgeley<sup>(3)</sup>. In principle a well-focused laser beam can produce a very good qualitative simulation of a hypervelocity impact because a large amount of energy is imparted onto a small target volume very quickly, followed by shock wave formation and crater formation. It is believed the latter two phenomena also occur in hypervelocity impacts.

In practice, as discussed in ref(3), the laser was used de-focussed in air, and the mechanism for imparting momentum would have been one of straightforward evaporation of target material by the laser energy. The technique still has the merit of imparting momentum very quickly (within 30ns), large signals could be obtained, the laser beam could be accurately aimed at the target, and reproducibility was very good (+10%). Using laser pulses therefore provided an excellent means of mapping the RAL mock-up shield.

#### 4. PRELIMINARY MAPPING OF THE UNCOATED SHIELD USING THE BMC

4.1 Before proceeding with the coating with CON-TACT and making a detailed laser mapping, a preliminary mapping of the shield was made using the BMC. The shield was stimulated at the same points that the SM shield had been so that a comparison of the two shield could be made.

The raw data obtained from these measurements is presented in table I. In order to compare these results with the SM measurements<sup>4)</sup> the same normalisations have been applied to the data and a comparison

with the SM data is presented in table II.

The same coordinate notation is used as in ref(4). The azimuthal direction is defined by numbering the rivets holding the stiffening ring in place, rivet number zero being defined as the one nearest to the +Y direction. The notation 60\*8 (say) would indicate 60 plus 8/12<sup>th</sup> rivet spacings from rivet number zero. As the rivets are uniformly spaced at 3° intervals this direction works out to be 180° from the +Y direction and is therefore the -Y direction. The radial position is defined by six standard distances from the inner edge designated A, S, B, C, D and E being 90mm, 150mm, 227mm, 350mm, 405mm and 520mm respectively.

There is reasonably good agreement between the mock-up shield data and the SM shield data at nearly every measured point on the shield, discrepancies between the mock-up shield data and the SM shield data being no worse than the discrepancies between the two sets of SM shield measurements. It is therefore concluded that the RAL mock-up shield is a good enough copy of the SM shield and presumably also the FM shield.

## 5. DETAILED LASER MAPPING ON COATED SHIELD

5.1 A system of polar coordinates was used to identify the laser impact points. The radial direction was defined as the number of mm from the inner edge of the shield. The practice used in the SM shield mapping of numbering the stiffening rings as an azimuthal reference was used again. Because the rivets on the mock-up shield are displaced one degree there is a systematic displacement equal to 1/3rd of a rivet spacing from between the azimuthal rotation used on the mock-up shield compared with that used on the SM shield. The +Y direction is designated as 0\*8 on the SM shield but as 0\*4 on the mock-up shield. Likewise the DID4 sensor direction is designated as 90\*4 on the SM shield but as 90\*0 on the mock-up shield.

The laser energy was monitored on each shot by reflecting off a proportion of the laser power into a calorimeter. The laser conditions were kept constant during the mapping to keep shot-to-shot variation to a minimum. Taking a random sample of 36 shots from the 2173 recorded shots the mean monitored energy measures at  $110 \pm 9$  mJ. The multiplying factor for determining the energy on target is 9.2 so the energy on target is determined as  $1.0 \pm 0.08$  mJ. Initially a minimum of two laser shots were fired at each laser position but eventually this policy was discontinued as it became apparent that shot-to-shot variability was within 10%. Henceforth only one shot was fired at each target point unless the laser power was outside the  $2\sigma$  limit.

The output from the flight-type piezo-electric sensors was passed through a 200kHz filter similar to the filters which comprise the first stage in the flight electronics, and the output from the filter recorded on an oscilloscope. A record was made of the data from each laser shot with the shots numbered in chronological order.

5.2 A summary of the mapping programme is given thus:

Record nos 1-311 first mapping of small sector before mis-location of inner stiffening ring was discovered.

Record nos 312-649 repeat mapping of small sector. Record no 409 was on 5 ms/sec time-base to determine the duration of the ringing round the inner stiffening ring. Record nos 645-649 determine the effect of hitting the inner stiffening ring connection to the small sector. Record nos 648-649 determine the effect of hitting a rivet.

Record nos 650-1341 mapping of the large sector from the DID2 joint to the conducting joint. Record nos 653-658 determine the effect of hitting rivets on the DID2 isolating joint. Shot nos 715-716 were directly onto DID2 sensors. Record nos 748-750 determine the effect of hitting an inner ring stiffening ring connection.

Record nos 1342-1912 mapping of the large sector from the DID3 joint to the conducting joint but omitting the area covered by the CIS. Shot nos 1392-1394 were directly on the DID3 sensor. Shot no 1410 was on a pillar connection, as were shot nos 1599-1602.

Record nos 1913-1935 mapping of the "ear"

Record nos 1936-2037 partial re-mapping of the large sector between the DID2 joint and the conducting joint.

Record nos 2095-2129 mapping of the CIS area. Holes 5mm in diameter were trepanned through the CIS at selected points so that the underlying shield could be stimulated. Thus the transmitting properties of the CIS area were directly measured without the complication of possible differences in the magnitude of the stimulation if the top layer of CIS is hit with laser pulses.

Record nos 2130-2135 shots were fired at selected points on top of the CIS to determine the effect of the CIS on the magnitude of the stimulation.

Record nos 2136-2151 mapping on the IPM

Record nos 2152-2159 shots on the "motor housing"

Record nos 2160-2171 further repeat mapping in the DID2 area

Record nos 2172-2173 repeat mapping in the DID3 area

## 6. THE DATA FILES

6.1 For each laser shot an oscilloscope trace was obtained on polaroid film of the response of each DID sensor. These traces were stuck on a record sheet, other relevant information about the laser shot written on, and the peak-to-peak maximum signal levels calculated and recorded on the record sheet. A sample record sheet is shown in figure 3. These record sheets, one for each laser shot, have been filed.

In order to manipulate the data more conveniently this data file has also been entered into computer storage. The data was stored and manipulated in the RAL casual users file CASTRO on the STARLINK

network.

The new data is stored in two data-files MAPPING and SHIELD. MAPPING contains record nos 1-311 in the following free format

record no

theta radius

monitor value

DID2 response: DID3 response: DID4 response

The data in this file is considered to be largely irrelevant due to the error in shield assembly mentioned in section 5 and this file will not be considered any further.

6.2 Record nos 312-2173 are stored in the sequential datafile SHIELD in the following free format

record no: theta: radius: monitor value: DID2 response: DID3

response: DID4 response

One line of datafile corresponds to one data record and the data is stored in order of ascending record number. For convenience in computation the hexadecimal azimuthal notation has been converted to decimal in the datafiles MAPPING and SHIELD. Thus an coordinate 17\*6 from the raw data files will have been recorded as 17.5 in the shield data file. The first stage in processing the data was to re-arrange the records according to the coordinate of the laser shot and the datafile RADSORT contains essentially the same data as SHIELD but with the lines re-arranged in ascending coordinate values. The shots in the IPM and motor housing are not included in this file. The DID responses contained in this file have been normalised to a monitor energy of 100mJ assuming a linear sensor response with energy.

Using RADSORT an averaged response of each sensor at each shield position was calculated and a new file named AVERAGED was entered into the computer. This file contains data records as follows

normalised      normalised      normalised  
theta: rad: DID2 response: DID3 response: DID4 response

The datafile LOGGED contains essentially the same information as AVERAGED but the sensor responses are in log form, normalised so that the log response on each sensor is 5.00.

- 6.3 In order to obtain a feeling for the two-dimensional response of each sensor three more datafiles designated DID2, DID3, and DID4 have been created. These contain the log responses of the designated sensor expressed as a rectangular array defined by the coordinates. Tables III, IV, V are print-outs of these files. Some data points have had to be omitted from these files where there is not room within the format to print-out all the datapoints available (eg close to the sensors). Also the mapping on the ear disappears, as it were, off the right hand side of the page in order to use the full width of print-out for the rest of the shield.

## 7. INTERPRETATION OF THE MAPPING DATA

- 7.1 There are two questions to be directed at the data.

1. Is it really representative of the FM shield?
2. How can it be used to deconvolute the shield response from the flight data?

Question no 1 is the more imponderable of the two because there can never be sufficient comparison data with the flight shield. The comparison of the uncoated mock-up shield with the SM shield gives confidence that the mock-up shield is a realistic copy of the FM shield, in so far that we believe the SM shield is also a realistic copy of the uncoated FM shield. The biggest uncertainty is whether the CON-TACT plastic layer adequately mimics the acoustical effect of the white paint coating on the flight shield.

- 7.2 Measurements on the FM shield are limited to two sets of measurements. J Zarnecki and R Turner have conducted one set using a piezo-electric stimulator and making analogue measurements directly

off the sensors, that is without a 200 kHz filter in the system. In order to make a comparison with these measurements the piezo-electric measurements of the DID2 response at a fixed distance of 227mm from the inside edge but with varying azimuth are plotted in figure 4. A similar plot is made of the RAL laser mapping responses at a distance of 241 mm. The responses obtained from the SM shield at 227 mm using bead drops is also plotted.

Not unexpectedly the addition of the CON-TACT plastic has caused an increase in the attenuating properties of the mock-up shield compared with the SM shield. There is now almost one order of magnitude further decay in making a complete traverse of the large sector.

However the FM measurements show the least attenuation of the three sets of measurements. This is surprising given that a white paint coated sample decay time was very much shorter than an uncoated sample (section 2). Since it is not likely, in the light of this experiment, that the white paint is actually reducing the attenuation on the FM shield these measurements would appear to indicate that either there is an appreciable difference between the FM and SM shields, or that the Zarnecki and Turner measurements are not representative of the attenuation of the FM shield.

As Zarnecki and Turner did not have a 200 kHz filter in the detecting system, it is possible that frequencies other than 200 kHz may not be attenuated as much by the shield and this could cause their measurements to show a lower apparent attenuation than actually occurs at 200 kHz. If this phenomenon exists it is investigatable on the mock-up shields.

7.3 The other set of data measurements on the FM shield consists of stimulation at a total of 11 points using BMC stimulation and using the flight electronics as the detecting system.

Table V shows the comparison of the DID2 FM data with the laser mapping data after the digital signals from the flight electronics have been converted to analogue voltage. The SM shield data is also included. For ease of comparison the results are normalised to 1.0 at 77\*5B.

It is difficult to draw firm conclusions from such a limited set of data, especially as some of the error bars are clearly large. However it would appear to support the Zarnecki and Turner set of measurements, in which case the RAL mock-up shield would be over-damped with the Fablon CON-TACT by an order of magnitude over the length of the large sector.

7.4 In answer to the second question it must be recalled that the objective with the MSM sensors is to measure masses to one order of magnitude. Particle events will be binned according to the apparent order of magnitude mass measured. In order to deconvolute the shield response function it is first necessary to evaluate what apparent variation in mass will occur over the shield area for one given event size. The next stage is to use this information to plot contours of equal apparent mass size on the shield at sufficiently close intervals. The contour map can then be used to calculate the areas of the shield corresponding to the various apparent mass bins. These areas give the probabilities of a given measured mass being in the various mass bins. The datafile LOGGED contains the raw data with which to do these calculations, which should be computerised. Time did not permit the author to computerise these calculations which were therefore partially done on a provisional basis using a hand calculator and manual plotting techniques.

The full contour map for DID2 response is shown in figure 5 and a contour map for the DID4 response over the isolated sector is shown in figure 6. The shield area versus response level is calculated

for DID2 in table VI and for DID4 in table VII. It is apparent from this table that deconvolution of the real masses from the apparent masses obtained from this sensor is likely to present a very real problem, and it is to be expected to be at least as bad for the DID3 sensor. This was however expected when the experiment in its present form was planned. It was also anticipated that the small sector would give a reasonably uniform response from the DID4 sensor and this has been realised in practice. On this scale, in which a shot direct on the sensor gives a log response 5.00, the whole sector is represented in the order of magnitude range 3.3 - 4.3 apart from a small area in the immediate vicinity of the sector and comprising only 0.9% of the total area. Because of the isolating properties of the shield the effective area of the next order of magnitude range down (2.3 - 3.3) is also very small. An examination of the DID4 datafile reveals that the area covered by the next range down (1.3 to 2.3) is about  $1\frac{1}{2}$  times the area of the small sector and the range below this covers most of the large sector. Since the number of dust particles is expected to fall off rapidly with increasing mass this should produce errors of only a few percent in the raw data figures received by DID4.

It would therefore appear that the DID4 channel will give good results even using the raw data, with the shield mapping providing the possibility of improving them further by deconvolution.

## 8. INTERPRETATION OF THE "SPECIAL SHOTS" DATA

8.1 The term special shots is used to include shots in special locations ie on rivets, inner stiffening ring supports, the IPM, the CIS top layer and the motor housing.

### 8.2 Rivet shots

Comparison of shots where a rivet is hit with those where the nearby shield is hit indicate that the response to a rivet shot is a factor

2 - 3 lower than hitting the nearby shield. In view of the small total area covered by the rivets this effect can probably be safely ignored.

### 8.3 Shots on inner stiffening ring supports

Shots on these areas show a similar size effect as shots onto rivets, but there was less reproducibility in the results. This is probably because the first laser shot into these fibreglass areas removes the top layer of plastic reinforcing making the response to the second shot different. However the stiffening ring supports only cover a small area and this effect can also probably be safely ignored.

### 8.4 The IPM mapping

The IPM mapping is documented in the datafile SHIELD. At a laser energy of 1J on target the responses of the DID2 sensor were in the region of 0.1mV, those of the DID3 sensor in the region of 0.2mV and of the DID4 sensor in the region of 0.5mV. This is to be compared to responses typically around 100mV for the DID4 sensor to shots in the small sector. The effect of impacts on to IPM for the MSM sensors is therefore small but possibly worth correcting for in the data reduction.

### 8.5 Shots on the CIS top layer

Six shots were fired on the CIS top layer at a distance of 241mm from the inner edge of the shield. The results from these shots are presented in table VIII interspersed between shots fired through holes in the CIS layer onto the underlying shield. These shots were also at a distance of 241mm from the inside edge. There is no discernable trend for the shots on the top layer to be significantly higher or lower than those onto the underlying shield. This would appear to indicate that the CIS does not have a significant effect on the magnitude of bending waves initiated by an impact onto it. However the attenuating effect in flexural waves propagating through

the CIS is very apparent.

#### 8.6 Shots on the "motor housing"

These shots are documented in the SHIELD datafile. They show that leakage at the 2 - 3% level occurs when the housing is hit in the vicinity of an inner ring support clamp which is also near one of the large sector sensors, and at the 5 - 10% level for hits near the support clamp close to DID4. This is a sufficiently large effect that some account should be taken of it in the data analysis.

Whilst not strictly within the bounds of "special shots" it should be noted that there is a leakage path across the isolating joints via the inner stiffening ring. It will be noted from the DID4 datafile print-out how much higher the DID4 response is to impacts at the inner edge of the large sector compared with further out.

This leakage path is sufficiently large that the signals from DID3 from this route are greater than those for the longer route around the large sector for shots which are on the large sector but are on the inner edge near the DID2 joint.

### 9. SUMMARY

9.1 The results from the laser mapping of the RAL mock-up shield have been presented. The way to use the data to obtain a function to deconvolute the shield responses from the raw acquisition data has been indicated.

Comparison with the SM shield data indicates that the mock-up shield is a realistic copy of the flight shield in most respects.

Comparison with the (limited) mapping data from the FM shield indicates the attempt to simulate the white coat paint finish of the FM shield may not have been completely successful. Further work on mock-up shields would be desirable to attempt to clarify this situation.

An assessment has been made of other factors eg hits on the motor

housing and the IPM which might influence the results obtained from the MSM sensors.

10. Acknowledgements

The author would like to thank B C Fawcett for the use of his laser for this work, especially appreciated as this has meant a postponement of his line identification experimental programme during the DIDSY calibration work. He would also like to acknowledge the help of R F Turner, E Sawyer and A Dean for the design and construction of the mock-up shield. He would like to thank his collaborators at the University of Kent at Canterbury for the supply of peizo-electric sensors and for use of the BMC. He would also like to acknowledge the assistance of K Watson, sandwich course student, for his assistance in making mapping measurements.

## REFERENCES

1. McDonnell J A M, Grun E, Evans G C, Turner R F, Firth J G, Casey W C, Kuczera H, Alexander W M, Clark D H, Grard R J L, Hanner M S, Hughes D W, Igenbergs E, Lindblad B A, Manderville J C, Schekm G, Sekanina Z, ESA Report ESA SP-169 (1981)
2. Evans S T, MSc Thesis (1984) University of Kent at Canterbury
3. Reading D H, Ridgeley A RAL report RL-83-024 (1983)
4. Evans S, Ridgeley A RAL report RAL-85-019 (1985)
5. McDonnell J A M, J Sci Instr (J Phys E) 2, p1026 (1969)
6. Stanyukovich K P, J Expt & Theor Phys (USSR) 36 p1609 (1959)
7. McDonnell J A M, Alexander W M, Lyons P, Tanner W, Anz P, Hyde T, Chen A L, Stevenson T J, Evans S T, Proceedings of 1984 COSPAR meetings, Graz Adv Space Res 4, p297 (1984)
8. Burton W M, RAL report RL-82-030 (1982)

TABLE I

## RAW DATA

## FROM BMC MEASUREMENTS ON UNCOATED SHIELD

## BNC TESTS ON RAL MOCK-UP SHIELD

COORDS	DID2 (mV)	DID3 (mV)	DID4 (mV)
1*7 A	8.7 + 3.0	70 + 10	
S	12 + 1.5	59 + 8.1	
B	5.4 + 0.70	49 + 16	
C	7.6 + 1.0	100 + 29	
D	9.0 + 2.6	73 + 1.7	
17*6 A	26 + 6.4	17 + 3.5	
S	27 + 4.5	16 + 1.7	
B	16 + 3.5	16 + 2.6	
C			
D			
E	11 + 1.9	13 + 3.3	
27*0A	31 + 3.5	16 + 3.1	
S	37 + 3.1	20 + 2.0	
B	37 + 3.1	23 + 8.5	
C			
D			
E	16 + 3.5	21 + 2.3	
34*2A	40 + 2.3	18 + 2.1	
S	41 + 13	17 + 8.0	
B	67 + 16	18 + 2.1	
C	32 + 10	49 + 8.6	
D	29 + 4.2	32 + 8.0	
35*6A	110 + 10	7.5 + 1.3	
S	110 + 19	9.1 + 1.2	
B	130 + 20	6.4 + 1.1	
C			
D	110 + 29	5.1 + 1.9	
60*8A	130 + 19	4.3 + 1.0	
S	120 + 30	4.7 + 1.2	
B	570 + 67	4.5 + 0.09	
C	160 + 22	5.0 + 1.05	
D	99 + 17	5.9 + 1.9	
77*5A	210 + 23	3.2 + 0.46	
S	190 + 12	3.2 + 0.23	
B	400 + 49	3.3 + 0.90	
C	450 + 10	4.4 + 0.68	
81*10A	170 + 23	2.5 + 0.32	
S	400 + 150	2.7 + 0.42	
B	1400 + 100	5.2 + 0.12	
C	290 + 45	5.7 + 2.3	
D	210 + 29	2.9 + 0.47	

BMC TESTS ON RAL MOCK-UP SHIELD

COORDS	DID2 (mV)	DID3 (mV)	DID4 (mV)
83*10A			
S			
B			
C			
D			
85*2 A	0.69 + 0.12		120 + 16
S		0.96 + 0.38	98 + 30
B		0.97 + 0.11	160 + 21
C	1.1 + 0.59		160 + 96
D	2.1 + 0.32		260 + 80
90*4 A	1.2 + 0.2	2.55 + 0.45	670 + 73
S	1.25 + 0.05	1.9 + 0.2	525 + 83
B	2.0 + 0.4	2.0	460 + 78
C	1.4	1.7	310 + 13
D	1.3	1.5 + 0.3	140 + 23
95*6 A		1.5 + 0.35	19 + 7.4
S	1.4 + 0.058		8.8 + 1.4
B		2.7 + 1.0	150 + 49
C	0.735+ 0.025	1.6	120 + 35
D		0.75 + 0.19	100 + 36
96*10A			
S			
B			
C			
D			
98*10A	2.6 + 0.40	240 + 29	
S	2.4 + 0.29	300 + 25	
B	2.1 + 0.38	710 + 87	
C	3.6 + 0.76	200 + 25	
D	2.95 + 0.84	200 + 63	
103*3A			
S	2.2 + 0.31	230 + 21	
B	2.2 + 0.21	350 + 50	
C	3.7 + 0.32	360 + 36	
D	2.7 + 0.72	160 + 15	
109*0A	6.3 + 1.6	74 + 25	
S			
B			
C	4.7 + 1.3	340 + 50	

TABLE II

## COMPARISON OF RAL MOCK-UP SHIELD WITH SM SHIELD

BMC AND BEAD DROP ANALOGUE NORMALISED TO 1.0 AT "STANDARD" POINTS

77\*5B FOR DID2

103\*3B FOR DID3

90\*4B FOR DID4

COORDS	DID2			DID3			DID4		
	RAL	SM		RAL	SM		RAL	SM	
	BMC	BMC	BEAD	BMC	BMC	BEAD	BMC	BMC	BEAD
1*7 A	0.022		0.0295	0.20		0.091			
S	0.030	0.035		0.17	0.11				
B	0.0135	0.0225	0.0205	0.14	0.24	0.050			
C	0.019		0.0495	0.29		0.094			
D	0.0225	0.0345	0.018	0.21	0.19	0.094			
17*6A	0.065		0.051	0.049		0.0275			
S	0.0675	0.089		0.046	0.057				
B	0.040	0.155	0.061	0.046	0.018	0.030			
C		0.125	0.0815		0.044	0.0435			
D		0.0895	0.026		0.027	0.020			
E	0.0275	0.053	0.0185	0.037	0.020	0.0195			
27*0A	0.0775		0.0925	0.046		0.0235			
S	0.0925	0.14		0.057	0.022				
B	0.0925	0.19	0.0605	0.066	0.031	0.0255			
C		0.21	0.195		0.022	0.025			
D		0.074	0.025		0.017	0.018			
E	0.040	0.0755	0.024	0.060	0.010	0.010			
34*2A	0.10		0.12	0.051		0.018			
S	0.10	0.175		0.049	0.025				
B	0.17	0.435	0.195	0.051	0.019	0.018			
C	0.080			0.14					
D	0.0725	0.195	0.060	0.091	0.010	0.0145			
35*6A	0.275		0.245	0.021		0.0135			
S	0.275	0.555		0.026	0.0089				
B	0.325	0.78	0.19	0.018	0.0080	0.0115			
C									
D	0.275	0.36	0.074	0.015	0.0059	0.0096			
60*8A	0.325		0.51	0.012		0.00635			
S	0.30	0.585		0.013	0.0050				
B	1.4	2.7	1.4	0.013	0.0061	0.0086			
C	0.40		0.18	0.014		0.0082			
D	0.25	0.25	0.195	0.017	0.0036	0.00635			
77*5A	0.525		0.49	0.0091		0.0039			
S	0.475	0.395		0.0091	0.0023				
B	1.0	1.0	1.0	0.0094	0.0039	0.0040			
C	1.1			0.013					
D		0.45	0.235		0.0035	0.0043			
81*10A	0.425		0.65	0.0071		0.0042			
S	1.0			0.0077					
B	3.5	1.8	1.1	0.015	0.0032	0.00385			
C	0.725			0.016					
D	0.525		0.16	0.0083		0.0046			

COORDS	DID2			DID3			DID4		
	RAL	SM		RAL	SM		RAL	SM	
	BMC	BMC	BEAD	BMC	BMC	BEAD	BMC	BMC	BEAD
85*2A	0.0017		0.013			0.0073	0.26		0.45
S		0.0094		0.0027	0.0053		0.21	0.27	0
B		0.013	0.026	0.0028	0.0084	0.010	0.35	0.35	0.50
C	0.0075						0.35		
D	0.00525	0.0059	0.0067		0.0053	0.0050	0.57	0.34	0.17
90*4A	0.0030		0.010	0.0073		0.00795	1.5		
S	0.0031	0.0080		0.0054	0.090		1.1	1.1	
B	0.0050	0.0070	0.011	0.0057	0.0065	0.0089	1.0	1.0	1.0
C	0.0035	0.0077	0.013	0.0049	0.0076	0.010	0.67	0.63	0.87
D	0.00325	0.0098	0.0090	0.0043	0.0065	0.0068	0.30	0.42	0.38
95*6A			0.0085	0.0043		0.0075	0.041		0.42
S	0.0035	0.0057			0.0069		0.019	0.43	
B		0.0033	0.0089	0.0077	0.014	0.0096	0.033	0.27	0.31
C	0.0018			0.0046			0.26		
D		0.0024	0.0050	0.0021	0.0031	0.00395	0.22	0.26	0.12
98*10A	0.0065		0.0068	0.69		0.39			
S	0.0060			0.86					
B	0.00525	0.0029	0.00835	2.0	1.4	1.2			
C	0.0090			0.57					
D	0.0074		0.00885	0.57		0.40			
103*3A									
S	0.0055	0.00465		0.66	0.76				
B	0.0055	0.0071	0.0079	1.0	0.90	1.0			
C	0.00925			1.0	1.0				
D	0.00675	0.00525	0.00735	0.46	1.1	0.50			
109*0A	0.016		0.023	0.21		0.13			
S									
B		0.0029	0.00915		0.37	0.26			
C	0.012	0.0029	0.016	0.97	0.58	0.67			
D		0.0024	0.011		0.40	0.325			

# TABLE III DID2 RESPONSE

	0	20	40	60	80	100	120	140	160	180	200	220	240	260	280	300	320	340	360	380	400	420	440	460	480	
89.5	2.00		1.64		1.51		1.55		1.68		1.56		1.55		1.53		1.42		1.50		1.62		1.49			
90.0		1.56	1.57	1.60	1.48																					
90.5	1.77		1.39		1.58		1.56		1.22		1.53		1.33		1.53		1.58		1.48		1.62		1.59			
91.0																										
91.5	1.62		1.75		1.37		1.56		1.66		1.65		1.75		1.53		1.59		1.48		1.57		1.53			
92.0																										
92.5	1.77		1.51		1.51		1.37		1.76		1.65		1.85		1.58		1.62		1.63		1.50		1.64			
93.0																										
93.5	1.57		1.52		1.47		1.42		1.45		1.55		1.52		1.56		1.43		1.58		1.49		1.47			
94.0																										
94.5	1.66		1.41		1.42		1.45		1.22		1.51		1.41		1.41		1.41		1.37		1.39		1.46			
95.0																										
95.5	1.50		1.34		1.22		1.28		1.31		1.28		1.31		1.23		1.36		1.44		1.65		1.48			
96.0	1.45		0.81		0.67		0.85		0.71		0.56	0.50	0.45	0.49	0.69		0.72		0.75		1.00		0.85			JOINT
96.5	1.64		0.97		1.05		0.81		0.92		0.77	1.03	1.11	1.07	0.97		1.29		1.13		1.05		1.18			
97.0										1.09	1.05	0.72	0.95	1.07	0.97											
97.5			1.20		1.15		1.07		1.22		1.05	0.97	1.23	1.23	1.03		1.31		1.31		1.29					
98.0									1.11		1.15	0.97	1.25		0.97						1.29					
98.5	1.33		1.13		0.95		1.11		0.95		0.92		1.13		0.95		0.97		1.05							
99.0																										
99.5	1.25		1.15		1.07		1.15		1.20		1.18		1.29		1.38		1.20		1.31		1.23					
100.0																										
100.5	1.33		1.18		1.13		1.00		1.11		1.18		1.23		1.13		1.18		1.47		1.15					
101.0																										
101.5	1.18		1.07		0.97		1.22		1.23		1.18		1.13		1.22		1.31		1.53		1.23		1.28			
102.0																										
102.5	1.20		1.00				1.13		1.17		1.13		1.26		1.22		1.33		1.45		1.22		1.11			
103.0																										
103.5	1.18						0.95		1.11		1.17		1.30		1.13		1.33		1.60		1.15		1.30			
104.0																										
104.5	1.25		1.42						1.05		1.13		1.09		1.23		1.17		1.62		1.39		1.20			
105.0																										
105.5	1.23		1.28		1.46				1.13		1.05		1.31		1.35		1.30		1.45		1.33		1.31			
106.0																										
106.5	1.26		1.55		1.41								1.17		1.31		1.13		1.31		1.28		1.34		1.13	
107.0																										
107.5	1.20		1.53		1.45								1.34		1.30		1.15		1.34		1.20		1.47			
108.0																										
108.5	1.34		1.54		1.38								1.22		1.25		1.49		1.66		1.29		1.49			
109.0																										
109.5	1.15		1.47		1.51								1.25		1.40		1.42		1.53		1.50		1.25			
110.0																										
110.5	1.43		1.70		1.54								1.26		1.49		1.63		1.53		1.38		1.46			
111.0																										
111.5	1.38		1.69		1.77								1.68		1.67		1.71		1.30		1.52		1.46		1.09	
112.0																										
112.5			1.69		1.73		1.76		1.70		1.65		1.66		1.76		1.53		1.56		1.63		1.41			
113.0																										
113.5	1.52		1.66		1.69		1.88		1.67		1.67		1.65		1.50		1.67		1.71		1.58		1.52			
114.0																										
114.5	1.56		1.59		1.56		1.88		1.88		1.56						1.59		1.85		1.44		1.55			
115.0																										
115.5	1.53		1.65		1.65		1.95		1.77		1.85						1.53		1.53		1.47		1.58			
116.0																										
116.5	1.39		1.58		1.81		1.85		1.77		1.63		1.60		1.54		1.51		1.60		1.43		1.54			
117.0													1.60													
117.5																										
118.0																										
118.5	1.30		1.66		1.68		1.88		2.00		1.67		1.61		1.77		1.61		1.81		1.49		1.55			
119.0													1.71													
119.5	1.49		1.95		1.85		1.88												1.85		1.77		1.85			

HOLE

IPM

}

120.0  
120.5  
1.0  
1.5  
2.0  
2.5  
3.0  
3.5  
4.0  
4.5  
5.0  
5.5  
6.0  
6.5  
7.0  
7.5  
8.0  
8.5  
9.0  
9.5  
10.0  
10.5  
11.0  
11.5  
12.0  
12.5  
13.0  
13.5  
14.0  
14.5  
15.0  
15.5  
16.0  
16.5  
17.0  
17.5  
18.0  
18.5  
19.0  
19.5  
20.0  
20.5  
21.0  
21.5  
22.0  
22.5  
23.0  
23.5  
24.0  
24.5  
25.0  
25.5  
26.0  
26.5  
27.0  
27.5  
28.0  
28.5  
29.0  
29.5  
30.0  
30.5  
31.0

C I S

120.5	1.74	1.85	2.00	2.18	1.97	1.69	1.73	1.81	1.77
1.0							1.88		
1.5	1.77	1.97	2.07	2.28					
2.0									
2.5	1.76	1.92	2.09	2.36	2.03	1.92	2.03	1.62	1.97
3.0							1.95		
3.5	1.77	1.81	2.13	2.37					
4.0									
4.5	1.88	1.97	2.05	2.36	2.30	2.17	2.11	2.17	2.05
5.0							2.00		
5.5									
6.0									
6.5	2.00	2.11	2.22	2.26	2.46	2.58	2.37	2.28	2.15
7.0							2.07		
7.5									
8.0									
8.5	1.81	1.92	2.05	2.54	2.65	2.64		2.34	2.50
9.0									
9.5					2.53	2.31	2.30	2.33	2.33
10.0									
10.5	2.00	1.92	2.05	2.34	2.28	2.50	2.22	2.25	2.20
11.0									
11.5		2.00	2.13	2.50	2.39	2.55	2.36	2.31	2.18
12.0									
12.5	2.20	2.09		2.18	2.29	2.31	2.95	2.56	2.36
13.0									
13.5	2.33			2.29	2.52	2.60	2.81	2.39	2.56
14.0									
14.5	2.26	2.61		2.53	2.73	2.58	2.62	2.85	2.51
15.0									
15.5	2.26	2.29	2.29	2.50	2.41	2.34	2.57	2.36	2.48
16.0									
16.5	2.31	2.37	2.30	2.51	2.40	2.66	2.43	2.56	2.60
17.0									
17.5	2.25	2.51	2.39	2.53	2.48	2.62	2.31	2.63	2.77
18.0									
18.5									
19.0									
19.5	2.13	2.53	2.49	2.34	2.44	2.49	2.59	2.59	2.62
20.0									
20.5									
21.0									
21.5	2.34	2.62	2.53		2.72	2.59	2.61	2.72	2.81
22.0									
22.5									
23.0									
23.5	2.48	2.49	2.54	2.69	2.58	2.58	2.61	2.63	2.42
24.0									
24.5									
25.0									
25.5	2.50	2.53	2.60	2.48	2.65	2.81	2.81	2.55	2.85
26.0									
26.5									
27.0									
27.5	2.33	2.58	2.53	2.66	2.70	3.00	2.72	3.05	2.54
28.0									
28.5									
29.0									
29.5	2.20	2.45	2.57	2.65	2.67	2.81	3.05	2.88	2.56
30.0									
30.5									
31.0									

1.95	1.63
1.65	1.60
1.74	
2.05	2.03
1.81	
2.00	1.95
1.73	
2.31	2.05
1.73	
2.15	1.92
2.00	
1.97	1.92
1.87	1.87
2.47	1.85
1.97	
2.44	1.77
1.88	
2.44	1.66
2.05	

HOLE

HOLE

1.81	1.41
1.54	1.66
1.62	1.81
1.73	1.81
EAR	
1.76	2.00
1.92	2.05
1.81	
2.15	2.17

31.5	2.25	2.61	2.67	2.59	2.81	2.55	2.88	2.85	2.81	2.58		
32.0												
32.5												
33.0												
33.5	2.28	2.46	2.71	2.67	2.48	3.03	2.97	2.92	2.76	2.55	2.51	2.57
34.0												
34.5	2.36	2.38	2.62	2.64	2.95	3.15	2.85	2.97	2.88	2.81	2.57	2.49
35.0	2.88	2.97	2.95	2.81	3.11	3.54	3.33	3.07	3.13	3.03	3.11	3.30
35.5												
36.0												
36.5	2.68	2.81	2.67	2.88	2.95	3.03	3.40	3.41	2.97	3.13	3.11	3.17
37.0												
37.5												
38.0												
38.5												
39.0												
39.5	2.74	2.95	2.81	2.81	3.05	3.17	3.56	3.45	3.11	3.13	3.11	3.03
40.0												
40.5												
41.0												
41.5	2.73	2.81	2.81	2.81								
42.0												
42.5	2.65	2.64		2.92	3.15	3.11	3.31	3.53	3.33	3.21	3.03	3.23
43.0												
43.5	2.85			2.95								
44.0												
44.5	2.88	3.13		3.26								
45.0												
45.5	2.88	3.03	3.00	3.09	3.15	3.20	3.23	3.28	3.39	3.25	3.43	3.40
46.0												
46.5												
47.0												
47.5												
48.0												
48.5	2.81	3.22	3.31	3.25	3.35	3.40	3.57	3.33	3.57	3.63	3.38	3.49
49.0												
49.5												
50.0												
50.5												
51.0												
51.5	2.95	3.17	3.22	3.23	3.44	3.57	3.22	3.58	3.92	3.56	3.17	3.20
52.0												
52.5												
53.0												
53.5						3.85	3.37	3.88	3.68	3.50		
54.0												
54.5	3.11	3.11	3.31	3.29	3.54	3.72	2.54	2.63	2.59	3.63	3.07	3.07
55.0												
55.5					3.25	3.68		2.57		3.39		
56.0												
56.5					3.29	2.65	2.69	2.62	2.62	3.54		
57.0												
57.5	3.30	3.39	3.34	3.41	3.33	2.62	2.88	2.65	2.85	3.28		
58.0												
58.5					3.18	3.58	3.85	3.37	3.34	3.33	3.17	3.03
59.0												
59.5												
60.0												
60.5	3.20	3.31	3.13	3.54	3.30	3.58	3.56	3.48	3.59	3.26	3.11	3.23
61.0												
61.5												
62.0												
62.5												

JOINT

HOLE

ANTENNA



# TABLE IV DID3 RESPONSE

	0	20	40	60	80	100	120	140	160	180	200	220	240	260	280	300	320	340	360	380	400	420	440	460	480
89.5	1.51		1.55		1.53		1.68		1.72		1.65		1.45		1.61		1.50		1.56		1.51		1.68		
90.0		1.53	1.43	1.68	1.49																				
90.5	1.57		1.65		1.68		1.72		1.44		1.57		1.30		1.61		1.65		1.72		1.57		1.44		
91.0																									
91.5	1.75		1.38		1.48		1.68		1.75		1.91		1.51		1.61		1.61		1.87		1.48		1.49		
92.0																									
92.5	1.48		1.65		1.42		1.61		1.72		1.80		1.68		1.80		1.89		1.72		1.61		1.65		
93.0																									
93.5	1.68		1.55		1.75		1.77		1.85		1.80		1.75		1.77		1.72		1.68		1.61		1.61		
94.0																									
94.5	1.75		1.61		1.57		1.91		1.80		1.93		2.11		1.83		1.80		1.46		1.57		1.51		
95.0																									
95.5	1.72		1.72		1.75		1.77		1.97		2.41		2.19		1.98		2.11		1.72		1.57		1.48		
96.0	3.16		2.83		3.02		3.17		3.55		3.56	3.77	3.91	3.68	3.29		2.95		3.03		3.06		3.28		JOINT
96.5	3.53		3.65		3.68		3.57		3.72		4.08	4.23	4.21	3.91	3.54		3.65		3.34		3.65		3.83		
97.0										3.83	3.93	4.50	4.00	3.80	3.65										
97.5			3.51		3.65		3.65		3.65		3.91	4.31	3.95	3.52	3.40		3.42		3.50		3.38				
98.0									3.65		4.13	4.26	4.15		3.57						3.38				
98.5	3.61		3.54		3.61		3.65		3.83		3.97		4.16		3.77		3.30		3.29						
99.0																									
99.5	3.65		3.65		3.53		3.83		3.95		3.93		4.16		3.83		3.65		3.40		3.36				
100.0																									
100.5	3.72		3.65		3.68		3.83		3.85		3.85		4.08		3.77		3.55		3.40		3.52				
101.0																									
101.5	3.55		3.65		3.83		3.80		3.77		3.87		4.02		3.97		3.72		3.61		3.29		3.72		
102.0																									
102.5	3.52		3.57				3.77		3.65		3.83		3.98		3.91		3.72		3.50		3.13		3.40		
103.0																									
103.5	3.38						3.29		3.75		3.77		3.93		3.93		3.83		3.72		3.48		3.14		
104.0																									
104.5	3.09		3.32						3.51		3.65		3.77		3.83		3.65		3.77		3.25		3.21		
105.0																									
105.5	3.09		3.33		3.20				3.36		3.54		3.87		3.80		3.80		4.03		3.31		3.29		
106.0																									
106.5	3.13		3.11		3.21								3.54		3.72		3.68		4.00		3.03		3.11		2.98
107.0																									
107.5	3.14		3.40		3.23								3.61		3.77		3.68		3.89		3.14		3.15		
108.0																									
108.5	3.02		3.04		3.09								3.80		3.57		3.57		3.72		3.22		3.17		
109.0																									
109.5	3.02		3.06		2.89								3.72		3.72		3.75		4.03		3.23		3.53		
110.0																									
110.5	3.19		2.98		3.08								3.68		3.65		3.61		3.61		3.03		3.40		
111.0																									
111.5	3.08		3.11		3.02								3.13		3.42		3.53		3.32		3.17		3.17		3.05
112.0																									
112.5			2.93		2.97		3.09		3.03		3.14		3.72		3.35		3.25		3.30		3.26		3.32		
113.0																									
113.5	2.65		3.01		2.95		2.77		2.95		3.06		3.72		3.24		3.54		3.38		3.08		3.36		
114.0																									
114.5	2.65		2.87		2.97		3.09		3.09		3.25						3.30		3.65		3.16		3.16		
115.0																									
115.5	2.75		2.87		2.97		2.85		2.77		3.42						3.18		3.36		3.33		3.09		
116.0																									
116.5	2.65		2.89		3.20		2.87		2.87		2.87		2.93		3.56		3.43		3.05		3.29		3.11		3.08
117.0															3.46										
117.5																									
118.0																									
118.5	2.93		2.93		2.87		3.02		2.77		3.02		3.33		3.23		2.91		3.15		2.97		3.05		
119.0															3.17										
119.5	2.75		2.83		2.91		2.80												3.29		3.17		3.15		

HOLE

IPM

}  
 2.87 2.93 3.56 3.43 3.05  
 3.46  
 2.77 3.02 3.33 3.23 2.91  
 3.17

120.0 :  
 120.5 :  
 1.0 :  
 1.5 :  
 2.0 :  
 2.5 :  
 3.0 :  
 3.5 :  
 4.0 :  
 4.5 :  
 5.0 :  
 5.5 :  
 6.0 :  
 6.5 :  
 7.0 :  
 7.5 :  
 8.0 :  
 8.5 :  
 9.0 :  
 9.5 :  
 10.0 :  
 10.5 :  
 11.0 :  
 11.5 :  
 12.0 :  
 12.5 :  
 13.0 :  
 13.5 :  
 14.0 :  
 14.5 :  
 15.0 :  
 15.5 :  
 16.0 :  
 16.5 :  
 17.0 :  
 17.5 :  
 18.0 :  
 18.5 :  
 19.0 :  
 19.5 :  
 20.0 :  
 20.5 :  
 21.0 :  
 21.5 :  
 22.0 :  
 22.5 :  
 23.0 :  
 23.5 :  
 24.0 :  
 24.5 :  
 25.0 :  
 25.5 :  
 26.0 :  
 26.5 :  
 27.0 :  
 27.5 :  
 28.0 :  
 28.5 :  
 29.0 :  
 29.5 :  
 30.0 :  
 30.5 :  
 31.0 :

C I S

120.5	2.40	2.87	2.97	2.72	2.56	2.77	2.91	2.61	2.77		3.00	2.72
1.0							3.10					
1.5	2.52	2.68	2.75	2.61						3.17	2.72	2.87
2.5	2.57	2.68	2.68	2.72	2.77	2.57	2.80	2.72	2.85	3.26	2.57	2.93
3.0							2.52					
3.5	2.77	2.61	2.68	2.53						3.00	2.85	2.89
4.5	2.77	2.61	2.68	2.46	2.65	2.29	2.43	2.61	2.72	3.16	2.95	2.75
5.0							2.40					
6.5	2.49	2.75	2.44	2.50	2.48	2.17	2.15	2.36	2.72	3.22	2.75	2.83
7.0							2.05					
8.5	2.19	2.57	2.57	2.47	2.42	2.35		2.40	2.59	3.03	3.06	2.68
9.5						2.43	2.30	2.42	2.42	2.83	3.01	2.68
10.5	2.44	2.47	2.50	2.40	2.50	2.43	2.31	2.51	2.45	2.87	2.80	2.80
11.5		2.52	2.72	2.68	2.29	2.53	2.43	2.26	2.30	2.83		
12.5	2.41	2.61		3.21	2.37	2.44	2.50	2.65	2.44	2.89	2.13	1.93
13.5	2.42			2.47	2.55	2.55	2.47	2.43	2.39	2.89		
14.5	2.28	2.44		2.26	2.68	2.34	2.57	2.68	2.30	2.87	1.85	1.89
15.5	2.00	2.29	2.18	2.19	2.47	2.40	2.68	2.52	2.37	2.93		
16.5	2.15	2.14	2.19	2.23	2.21	2.40	2.36	2.45	2.29	2.87		
17.5	2.11	2.22	2.36	2.22	2.36	2.40	2.48	2.46	2.57	2.83	1.85	1.89
19.5	1.97	2.25	2.21	2.26	2.15	2.11	2.40	2.39	2.55	2.97		
20.5											1.85	1.77
21.5	2.06	2.06	2.17		2.00	2.41	2.40	2.27	2.21	2.75		
23.5	1.83	1.97	2.06	2.13	2.15	2.18	2.29	2.19	2.39	2.61		
24.5											1.80	1.75
25.5	1.83	2.06	2.13	2.00	2.19	2.06	2.25	2.16	2.46	2.46		
27.5	1.85	2.13	2.05	2.03	2.23	2.06	2.17	2.20	2.44	2.75	1.57	1.65
29.5	1.80	2.09	2.05	2.00	2.05	2.16	2.16	2.08	2.25	2.56	1.56	
31.0											1.68	1.68

HOLE

HOLE

2.13	1.93
1.85	1.89
1.85	1.89
1.85	1.77
EAR	
1.80	1.75
1.57	1.65
1.56	
1.68	1.68

63 0															
63 5	0.87	1.13	1.08	1.09	1.17	0.95	0.93	1.15	1.28	1.10	0.87	0.89			
64 0															
64 5															
65 0															
65 5															
66 0															
66 5	0.87	1.02	1.03	0.98	1.17	1.28	1.10	0.95	1.15	0.98	0.75	0.75			
67 0															
67 5															
68 0															
68 5	0.80	1.05	1.03	1.06	1.37	1.14	1.13	1.30	1.29	1.40	0.83	0.89			
69 0															
69 5															
70 0															
70 5	0.98	1.11	1.17	1.08	1.10	1.33	1.11	1.03	0.89	1.05	0.65	0.80			
71 0															
71 5	0.93	0.93	1.09	0.95											
72 0															
72 5	0.93	0.95		1.17	1.00	1.21	1.22	1.20	1.57	1.40	0.98	0.72			
73 0															
73 5	0.87	0.89		0.98											
74 0															
74 5	0.75	0.85		0.77	1.06	1.09	1.10	1.17	1.21	1.42	0.91	0.72	0.52		
75 0															
75 5	0.61	0.77	0.83	0.83	0.89										
76 0															
76 5	0.77	0.85	0.98	1.03	1.05	0.93	1.00	1.16	1.16	1.54	0.65	0.57			
77 0															
77 5															
78 0															
78 5	1.03	0.77	0.80	0.80	0.89	0.77	1.03	1.00	1.06	1.31	0.77	0.65			
79 0															
79 5	1.09	0.93	0.87	0.89	0.97	1.10	1.09	1.15	1.27	1.16	0.57	0.77			
80 0															
80 5	0.95	0.77	0.91	1.05		1.00	0.97	1.02	0.93	0.97	1.10	1.11	0.85	0.57	0.65
81 0															
81 5	1.06	0.95	0.80		0.98	0.93	0.97		1.29	0.97	1.10	0.83	0.95		
82 0	1.08			1.10	0.75	1.02	1.03	0.75							
82 5		0.87	0.80	0.68	0.68	0.91	0.85	0.98	1.03	0.98	0.87	0.83	1.18	0.91	0.91
83 0						0.72	0.75	0.83	0.75	0.65	0.65	0.98			
83 5	1.14	0.72	0.77	0.85	0.83	0.95	0.89	0.87	0.91	0.80	1.15	0.65	0.61		
84 0	1.32	0.72	0.87	0.68	0.65	0.85	0.85	0.77	0.72	0.61	0.93	0.57	0.38		
84 5	1.61	1.59	1.36	1.27	1.18	1.06	1.09	1.35	1.25	1.40	1.47	1.45			JOINT
85 0															
85 5	1.77	1.57	1.47	1.43	1.53	1.42	1.51	1.37	1.48	1.49	1.31	1.36			
86 0															
86 5	1.61	1.46	1.50	1.57	1.48	1.45	1.57	1.65	1.46	1.48	1.42	1.28			
87 0															
87 5	1.54	1.61	1.57	1.61	1.61	1.57	1.36	1.49	1.75	1.54	1.26	1.29			
88 0															
88 5	1.68	1.61	1.72	1.44	1.65	1.45	1.36	1.45	1.38	1.48	1.54	1.57			
89 0															

HOLE

HOLE

JOINT

31.5	1.89	1.89	2.05	2.08	2.17	1.98	1.89	1.97	2.08	2.72		
32.0												
32.5												
33.0												
33.5	1.97	2.05	2.02	2.06	2.14	1.98	1.87	2.20	2.37	2.61	2.18	1.98
34.0												
34.5	2.25	1.93	1.75	1.75	1.93	1.72	1.85	1.83	1.97	2.20	2.33	1.93
35.0	1.45	1.91	1.72	1.89	1.77	1.85	1.61	2.06	1.91	2.00	1.65	1.65
35.5												
36.0												
36.5	1.27	1.61	1.54	1.65	1.52	1.68	1.57	1.45	1.51	1.83	1.50	1.45
37.0												
37.5												
38.0												
38.5												
39.0												
39.5	1.20	1.53	1.37	1.65	1.44	1.57	1.52	1.53	1.95	1.91	1.46	1.65
40.0												
40.5												
41.0												
41.5	1.52	1.68	1.47	1.33								
42.0												
42.5	1.31	1.45	1.42	1.43	1.51	1.61	1.51	1.57	1.72	1.44	1.45	
43.0												
43.5	1.34		1.36									
44.0												
44.5	1.45	1.27	1.37									
45.0												
45.5	1.23	1.38	1.27	1.30	1.57	1.57	1.56	1.44	1.61	1.65	1.20	1.25
46.0												
46.5												
47.0												
47.5												
48.0												
48.5	1.10	1.35	1.29	1.42	1.46	1.37	1.61	1.43	1.68	1.50	1.27	1.20
49.0												
49.5												
50.0												
50.5												
51.0												
51.5	1.15	1.34	1.15	1.27	1.47	1.36	1.47	1.44	1.35	1.53	1.38	1.54
52.0												
52.5												
53.0												
53.5						1.44	1.48	1.34	1.51	1.87		
54.0												
54.5	1.03	1.13	1.23	1.30	1.55	1.42	0.68	0.85	0.85	1.68	1.18	1.18
55.0												
55.5					1.36	1.14		0.80		1.68		
56.0												
56.5					1.42	0.77	0.72	0.68		1.52		
57.0												
57.5	1.20	1.39	1.26	1.30	1.09	0.57	0.75	0.57	0.68	1.65		
58.0												
58.5					1.17	1.06	1.10	1.22	1.49	1.57	0.95	0.97
59.0												
59.5												
60.0												
60.5	0.95	1.02	1.10	1.31	1.11	1.09	1.23	1.19	1.45	1.40	1.11	1.03
61.0												
61.5												
62.0												
62.5												

JOINT

HOLE

ANTENNA

# TABLE V DID4 RESPONSE

	0	20	40	60	80	100	120	140	160	180	200	220	240	260	280	300	320	340	360	380	400	420	440	460	480	
1.0													0.40													
1.5	1.10	0.91	1.08	0.74															0.68	0.55	0.76					
2.0																										
2.5	1.03	0.80	0.69	0.59	0.67	0.43	0.51	0.56	0.50										0.65	0.69	0.84					
3.0													0.23													
3.5	0.98	0.76	0.77	0.74															0.69	0.80	1.00					
4.0																										
4.5	1.00	0.65	0.63	0.84	0.36	0.33	0.26	0.43	0.52										0.55	0.71	0.62					
5.0													0.20													
5.5																			0.50	0.70	0.80					
6.0																										
6.5	0.98	0.73	0.88	0.46	0.57	0.42	0.39		0.12												0.66	0.73				
7.0													-0.05													
7.5																					0.60	0.80				
8.0																										
8.5	0.91	0.65	0.65	0.75	0.65	0.53			0.34	0.38	0.39	0.84	0.61													
9.0																										
9.5								0.62	0.49	0.45	0.39	0.44	0.48	0.69	0.64											
10.0																										
10.5	0.88	0.61	0.73	0.69	0.48	0.52	0.55	0.50	0.56	0.56	0.76	0.84														
11.0																										
11.5		0.61	0.61	0.70	0.58	0.56	0.55	0.43	0.47	0.52																
12.0																					0.28	0.03				
12.5	0.73	0.69		0.37	0.63	0.55	0.64	0.49	0.45	0.42																
13.0																										
13.5	0.64			0.43	0.71	0.56	0.61	0.54	0.65	0.56																
14.0																										
14.5	0.76	0.61		0.65	0.72	0.60	0.70	0.54	0.70	0.65											-0.12	0.03				
15.0																										
15.5	0.84	0.57	0.67	0.65	0.56	0.64	0.52	0.56	0.76	0.65																
16.0																										
16.5	0.77	0.64	0.59	0.64	0.56	0.63	0.45	0.50	0.37	0.42																
17.0																										
17.5	0.77	0.61	0.60	0.69	0.52	0.60	0.47	0.84	0.61	0.64												0.03				
18.0																										
18.5																										
19.0																										
19.5	0.84	0.70	0.63	0.61	0.50	0.41	0.44	0.54	0.32	0.37																
20.0																										
20.5																						0.03	0.06			
21.0																										
21.5	0.91	0.75	0.56	0.55	0.34	0.40	0.60	0.51	0.43																	
22.0																										
22.5																										
23.0																										
23.5	1.08	0.66	0.84	0.51	0.69	0.54	0.45	0.33	0.41	0.47																
24.0																										
24.5																										
25.0																										
25.5	0.82	0.80	0.56	0.58	0.62	0.49	0.61	0.48	0.47	0.64																
26.0																										
26.5																										
27.0																										
27.5	1.06	0.61	0.46	0.52	0.54	0.51	0.37	0.57	0.43	0.49												-0.12	0.08			
28.0																										
28.5																										
29.0																										
29.5	1.03	0.56	0.58	0.53	0.53	0.51	0.52	0.38	0.39	0.49													-0.10			
30.0																										
30.5																										
31.0																										

CIS

HOLE

HOLE

EAR

31.5	1.08	0.91	0.65	0.48	0.56	0.45	0.44	0.56	0.34	0.53		
32.0												
32.5												
33.0												
33.5	1.03	0.84	0.72	0.72	0.70	0.63	0.60	0.69	0.32	0.54	0.52	0.54
34.0												
34.5	0.84	0.76	0.29	0.56	0.42	0.58	0.61	0.51	0.51	0.61	0.48	0.38
35.0	0.74	0.91	0.74	0.63	0.68	0.91	0.61	0.75	0.64	0.90	0.95	0.98
35.5												
36.0												
36.5	1.00	0.74	0.72	0.70	0.78	0.74	0.88	0.72	0.77	0.74	0.70	0.91
37.0												
37.5												
38.0												
38.5												
39.0												
39.5	0.75	0.71	0.72	0.79	0.80	1.03	0.78	0.95	0.98	0.95	0.80	0.66
40.0												
40.5												
41.0												
41.5	1.12	0.62	0.59	0.72								
42.0												
42.5	0.80	0.65	0.58	0.58	1.00	0.77	0.98	0.84	0.98	1.06	0.84	0.80
43.0												
43.5	0.84		0.98	0.98								
44.0												
44.5	1.08	1.03	0.84	0.84								
45.0												
45.5	1.06	1.08	1.00	0.91	0.95	0.98	0.95	0.77	0.91	1.08	0.95	0.80
46.0												
46.5												
47.0												
47.5												
48.0												
48.5	1.23	0.98	1.00	1.08	1.14	1.21	1.18	1.06	1.06	1.06	1.06	1.00
49.0												
49.5												
50.0												
50.5												
51.0												
51.5	1.44	1.08	1.08	1.16	1.08	1.16	1.14	1.12	1.10	1.32	1.25	1.10
52.0												
52.5												
53.0												
53.5						1.08	1.12	1.23	1.23	1.18		
54.0												
54.5	1.18	1.36	1.18	1.16	1.28	1.16	1.06	0.80	1.08	1.28	1.36	1.03
55.0												
55.5					1.21	1.14		1.21		1.39		
56.0												
56.5					1.29	1.06	0.98	0.98	0.98	1.33		
57.0												
57.5	1.52	1.37	1.28	1.32	1.18	1.00	0.91	0.95	0.95	1.29		
58.0												
58.5					1.16	1.20	1.26	1.31	1.25	1.33	1.18	1.28
59.0												
59.5												
60.0												
60.5	1.42	1.34	1.32	1.20	1.20	1.23	1.32	1.29	1.28	1.25	1.21	1.23
61.0												
61.5												
62.0												
62.5												

HOLE

ANTENNA

JOINT



94.5	3.88	3.98	3.88	3.95	3.84	3.88	3.84	3.80	3.72	3.61	3.53	3.67		
95.0														
95.5	3.84	3.65	3.70	3.68	3.70	3.54	3.68	3.40	3.46	3.62	3.80	3.61	JOINT	
96.0	2.63	2.25	2.16	1.88	1.91	1.74	2.03	2.03	2.14	2.21	2.10	1.98	2.08	2.12
96.5	2.28	1.95	1.84	1.68	1.60	1.66	1.65	1.65	1.63	1.54	1.73	1.67	1.77	1.52
97.0						1.70	1.58	1.59	1.61	1.53	1.56			
97.5		1.84	1.70	1.54	1.68	1.59	1.53	1.59	1.52	1.45	1.55	1.56	1.65	
98.0					1.61	1.52	1.54	1.60		1.56			1.46	
98.5	1.84	1.68	1.59	1.71	1.66	1.59		1.47		1.69	1.53	1.33		
99.0														
99.5	1.84	1.78	1.55	1.66	1.76	1.63	1.53	1.55	1.50	1.63	1.65			
100.0														
100.5	1.80	1.72	1.73	1.54	1.66	1.61	1.63	1.34	1.61	1.50	1.42			
101.0														
101.5	1.71	1.70	1.84	1.69	1.68	1.61	1.66	1.48	1.54	1.56	1.63	1.59		
102.0														
102.5	1.88	1.65		1.54	1.44	1.58	1.65	1.61	1.44	1.50	1.53	1.28		
103.0														
103.5	1.84			1.55	1.53	1.58	1.65	1.52	1.54	1.47	1.44	1.41		
104.0														
104.5	1.78	1.54			1.49	1.44	1.45	1.48	1.37	1.41	1.41	1.28		
105.0														
105.5	1.70	1.46	1.36		1.33	1.36	1.52	1.49	1.34	1.52	1.47	1.55		
106.0														
106.5	1.73	1.44	1.42				1.33	1.33	1.23	1.54	1.38	1.33	1.23	
107.0														
107.5	1.62	1.49	1.71				1.49	1.51	1.28	1.25	1.38	1.25		
108.0														
108.5	1.56	1.43	1.38				1.31	1.46	1.34	1.46	1.34	1.37		
109.0														
109.5	1.46	1.34	1.63				1.43	1.31	1.36	1.36	1.36	1.31		
110.0														
110.5	1.58	1.33	1.44				1.12	1.47	1.40	1.08	1.28	1.36		
111.0														
111.5	1.42	1.44	1.28				1.12	1.06	1.29	1.00	1.00	1.26	0.88	
112.0														
112.5		1.08	1.29	1.10	1.10	1.00	1.06	1.12	1.21	1.21	1.08	1.16		
113.0														
113.5	1.43	1.18	1.06	0.98	0.91	0.68	1.06	1.00	1.12	1.08	1.03	1.36		
114.0														
114.5	1.36	1.12	1.03	1.00	1.10	1.18			1.16	1.16	0.98	1.14		
115.0														
115.5	1.25	1.03	0.98	0.88	0.88	1.08			1.14	1.00	1.14	1.10		
116.0														
116.5	1.23	1.06	0.98	0.80	0.91	0.72	0.91	0.99	1.00	0.88	1.03	0.77		
117.0							0.65							
117.5														
118.0														
118.5	1.10	0.95	0.98	0.74	0.68	0.51	0.71	0.70	0.80	0.73	1.00	0.95		
119.0							0.42							
119.5	1.18	1.16	0.95	0.77						0.69	0.84	0.79		
120.0														
120.5	1.06	1.00	0.95	0.74	0.60	0.42	0.40	0.68	0.74		0.75	0.84		

HOLE

IPM

CIS

63.0															
63.5	1.66	1.34	1.34	1.41	1.26	1.31	1.40	1.03	1.21	1.21	1.45	1.26			
64.0															
64.5															
65.0															
65.5															
66.0															
66.5	1.71	1.39	1.45	1.33	1.33	1.38	1.32	1.36	1.41	1.41	1.36	1.37			
67.0															
67.5															
68.0															
68.5	1.79	1.36	1.42	1.40	1.40	1.44	1.42	1.65	1.43	1.38	1.45	1.38			
69.0															
69.5															
70.0															
70.5	1.88	1.57	1.52	1.57	1.42	1.56	1.42	1.51	1.47	1.42	1.52	1.41			
71.0															
71.5	1.91	1.43	1.25	1.52											
72.0															
72.5	2.00	1.63		1.54	1.63	1.70	1.78	1.84	1.58	1.58	1.50	1.48			
73.0															
73.5	2.31	1.88		1.60											
74.0															
74.5	1.91	1.71		1.69	1.84	1.67	1.55	1.66	1.60	1.63	1.55	1.55	1.44		
75.0															
75.5	1.84	1.56	1.84	1.80	1.52										
76.0															
76.5	2.10	1.84	1.69	1.66	1.62	1.68	1.68	1.55	1.55	1.67	1.59	1.84			
77.0															
77.5															
78.0															
78.5	2.10	1.69	1.80	1.72	1.71	1.61	1.63	1.52	1.38	1.39	1.58	1.47			
79.0															
79.5	2.21	2.10	1.76	1.79	1.84	1.64	1.66	1.65	1.66	1.51	1.71	1.59			
80.0															
80.5	2.06	1.91	1.63	1.70											
81.0															
81.5	1.98	1.84	1.84		2.00	1.80	1.61	1.68	1.79	1.73	1.84	1.78			
82.0	2.34			1.72	1.78	1.77	1.84	1.71							
82.5		1.84	2.10	1.68	1.88	1.88	1.84	1.90	1.98	1.84	1.55	1.52	1.74	2.03	1.84
83.0					1.88	1.98	1.77	1.84	1.61	1.65	1.68				
83.5	2.33	1.95	1.88	1.72	1.95	1.91	2.18	2.00	1.63	1.88	2.00	2.06	1.98		
84.0	2.38	2.28	2.37	2.10	1.78	2.04	2.18	2.08	2.34	2.37	2.31	2.08			
84.5	3.63	3.88	3.79	3.41	3.31	3.36	3.31	3.56	3.58	3.75	3.76	3.68			JOINT
85.0															
85.5	3.66	3.68	3.84	3.68	3.79	3.80	3.75	3.68	3.80	3.84	4.03	3.98			
86.0															
86.5	3.58	3.58	3.80	3.98	3.95	3.84	3.88	3.84	3.79	3.82	3.88	3.77			
87.0															
87.5	3.74	3.79	4.03	3.98	3.98	3.88	3.84	3.84	3.84	3.91	3.91	4.00			
88.0															
88.5	4.23	4.06	4.06	4.10	4.03	3.98	3.91	3.91	3.80	3.88	3.56	3.54			
89.0															
89.5	4.42	4.21	4.23	4.20	4.12	4.06	3.88	3.77	3.80	3.75	3.60	3.65			
90.0		4.56	4.52	4.28	4.18										
90.5	3.95	4.16	4.06	4.08	3.88	3.95	3.65	3.80	3.74	3.98	3.58	3.60			
91.0															
91.5	4.12	4.00	4.06	4.00	3.91	3.91	3.78	3.74	3.79	3.98	3.50	3.61			
92.0															
92.5	3.95	4.08	3.95	3.98	3.98	3.91	3.95	3.74	3.72	3.70	3.56	3.57			
93.0															
93.5	3.88	4.03	4.08	3.91	3.84	3.95	3.84	3.75	3.73	3.63	3.44	3.64			
94.0															

HOLE

HOLE

JOINT

TABLE VI SHIELD AREA VERSUS RESPONSE LEVEL FOR DID2

RESPONSE LEVEL	SHIELD AREA %
4.25 - 5.00	0.20
4.00 - 4.25	1.3
3.75 - 4.00	5.0
3.50 - 3.75	8.8
3.25 - 3.50	14
3.00 - 3.25	7.3
2.75 - 3.00	5.0
2.50 - 2.75	11
2.25 - 2.50	5.7
2.00 - 2.25	3.3
1.75 - 2.00	9.4
1.50 - 1.75	16
1.25 - 1.50	7.9
1.00 - 1.25	<u>5.6</u>
	100.0 % TOTAL

TABLE VII SHIELD AREA VERSUS RESPONSE LEVEL FOR DID4

RESPONSE LEVEL	SMALL SECTOR AREA (%)
4.25 - 5.00	0.82
4.00 - 4.25	11
3.75 - 4.00	53
3.50 - 3.75	32
3.25 - 3.50	3.4

TABLE VIII COMPARISON OF SHOTS ON TOP LAYER OF CIS WITH NEARBY SHOTS ON UNDERLYING SHIELD

THETA COORDINATE	DID2 RESPONSE (mV)	DID3 RESPONSE (mV)	DID4 RESPONSE (mV)
116.5 B	0.68	98	0.13
117.0 T	0.67	78	0.071
118.5 B	0.69	58	0.081
119.0 T	0.88	40	0.042
120.5 B	0.92	22	0.040
1.0 T	1.3	34	0.040
2.5 B	1.8	17	0.051
3.0 T	1.5	9.0	0.027
4.5 B	2.2	7.3	0.029
5.0 T	1.7	6.8	0.025
6.5 B	4.0	3.8	0.039
7.0 T	2.0	3.0	0.014



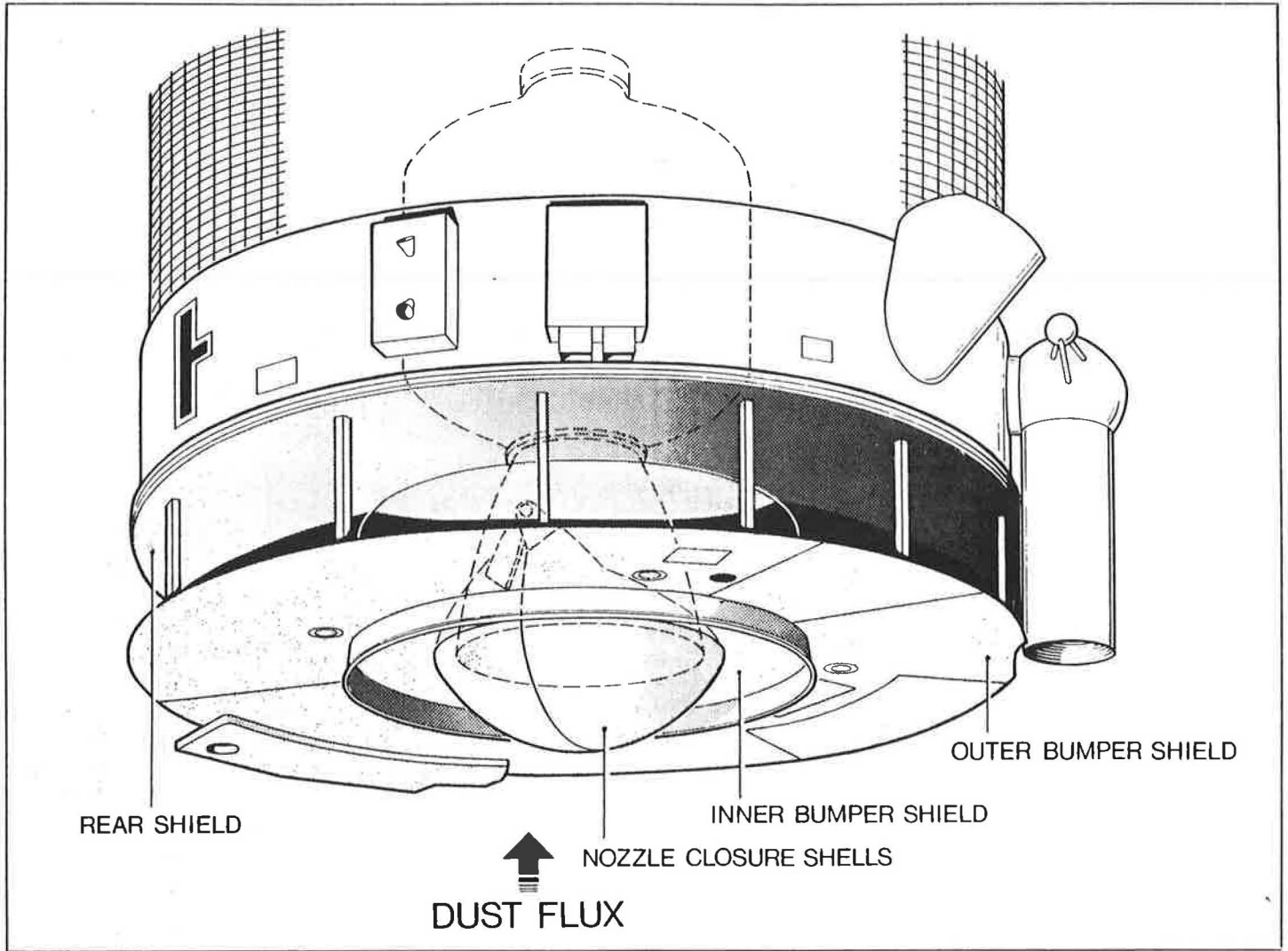


FIG.1 - Artist impression of Giotto's dust protection system (ESA Bulletin No.32 P.37)

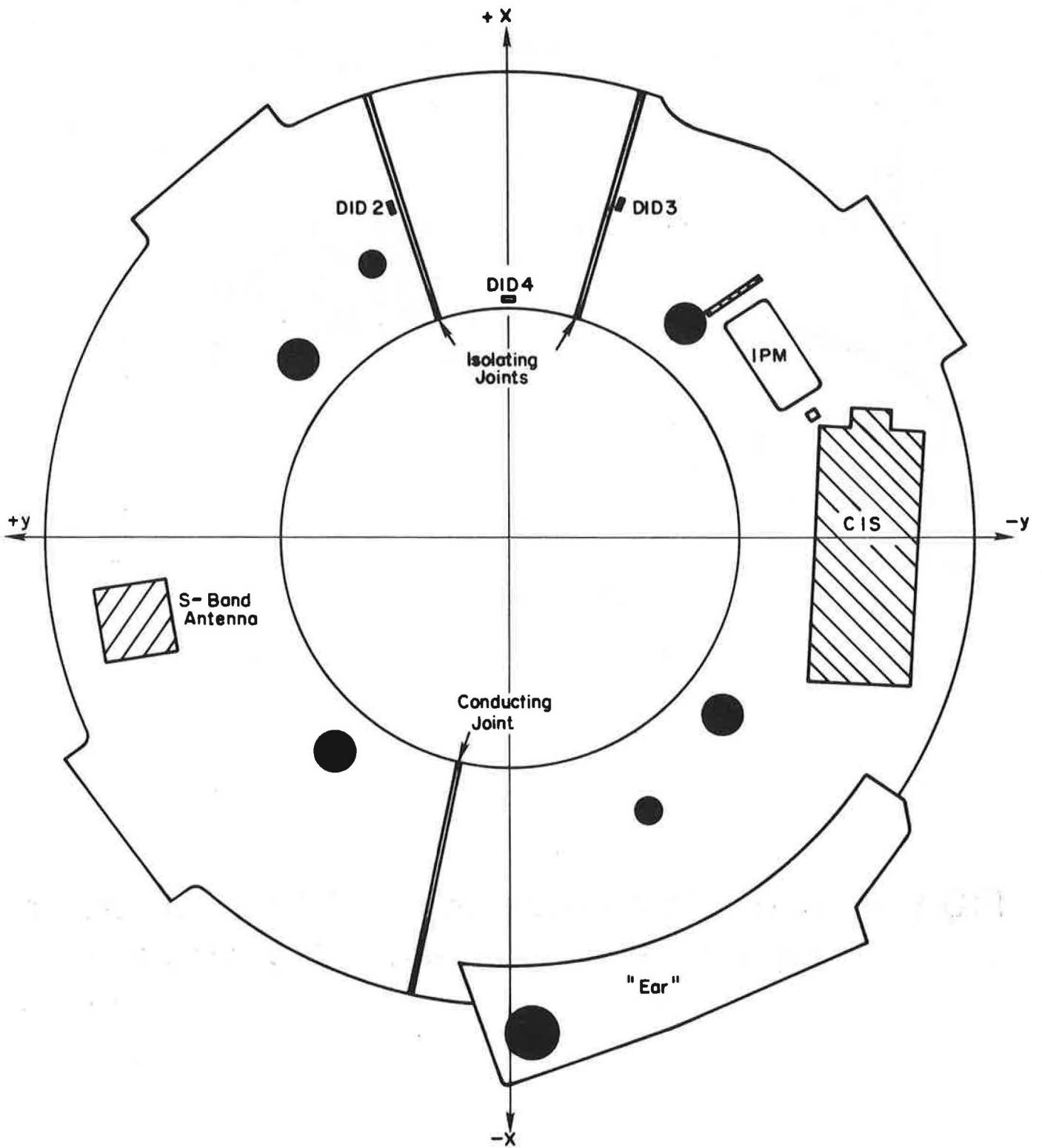


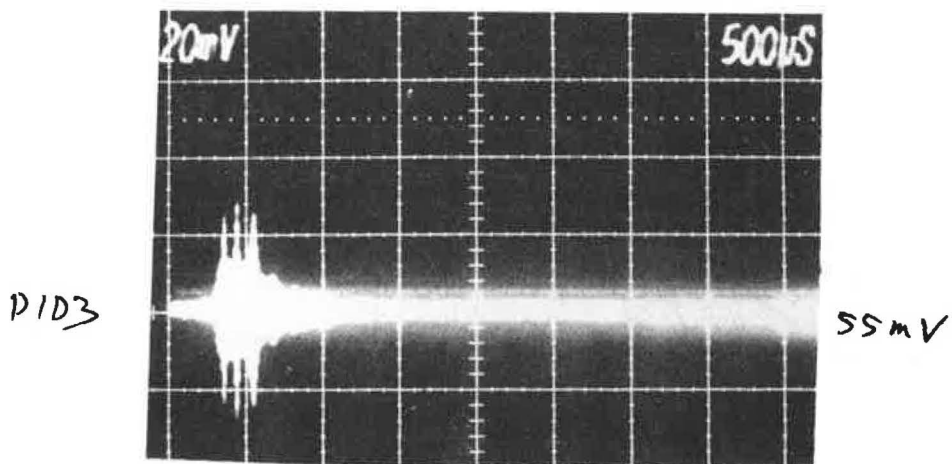
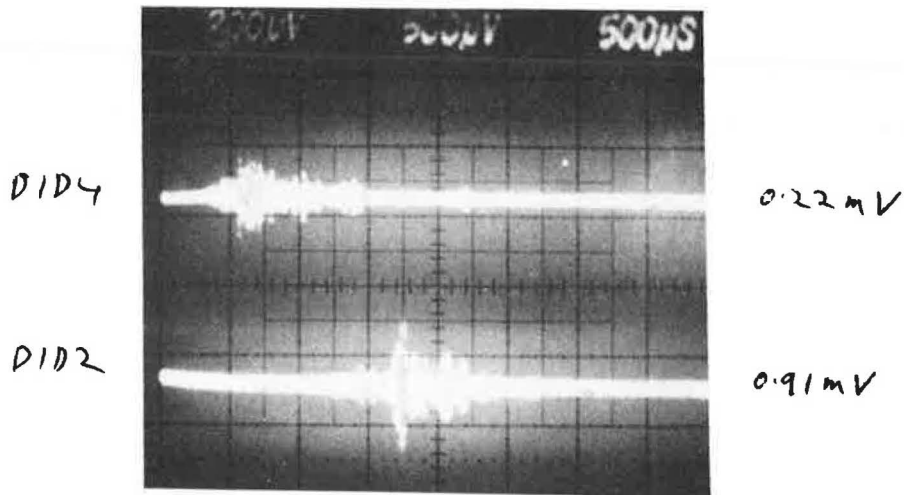
Fig. 2 The DIDSY Bumper Shield.

RECORD NO. 1590

DATE 17/9/84

SHIELD COORDS 112 \* 6 : 281

MONITOR 91 m J



COMMENTS

FIG.3 A SAMPLE DATA RECORD

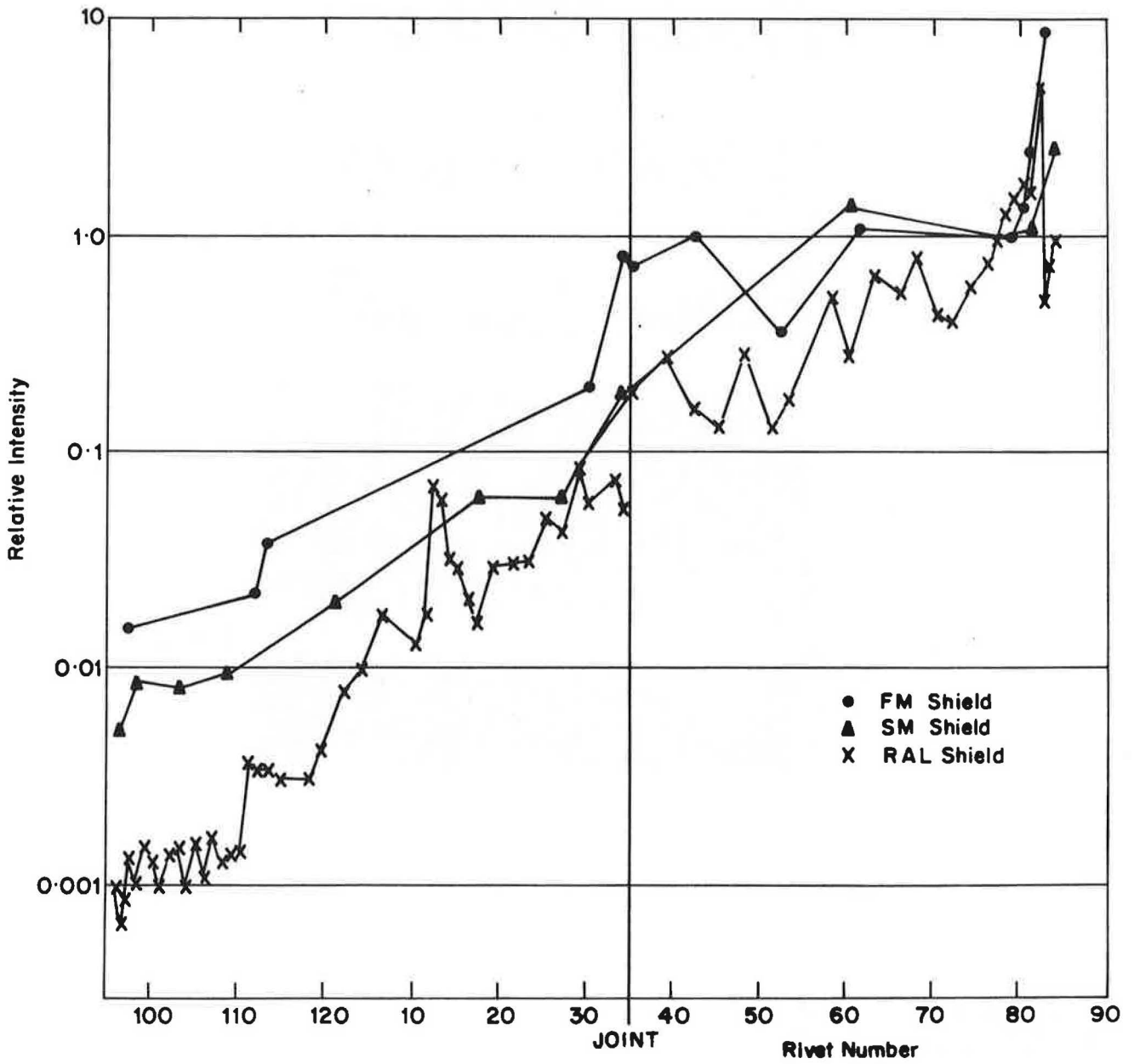


Fig.4 Comparison of DID2 Responses for the R.A.L. Mock-up, SM and FM Shields.

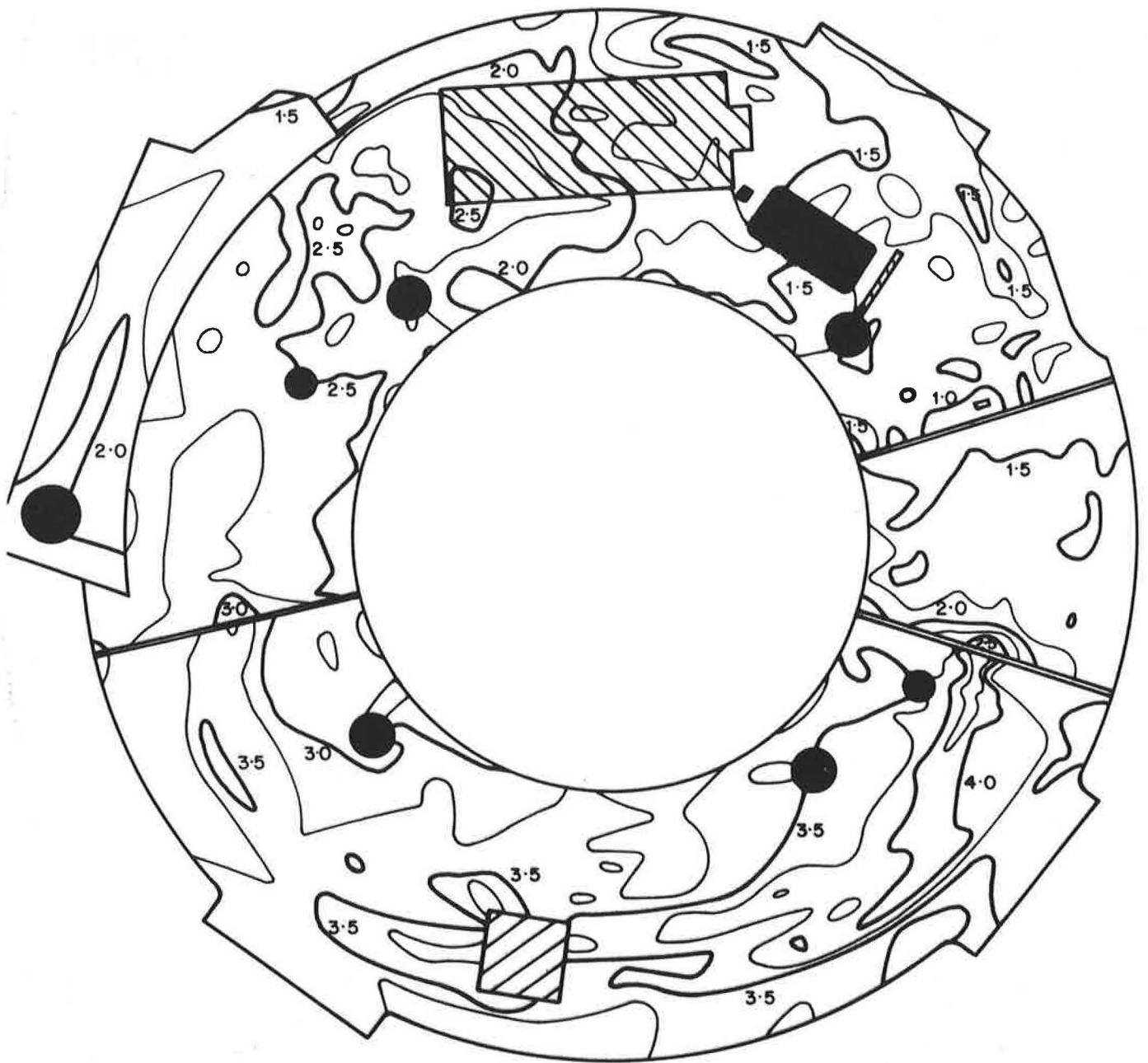


Fig.5 DID 2 Contour Map

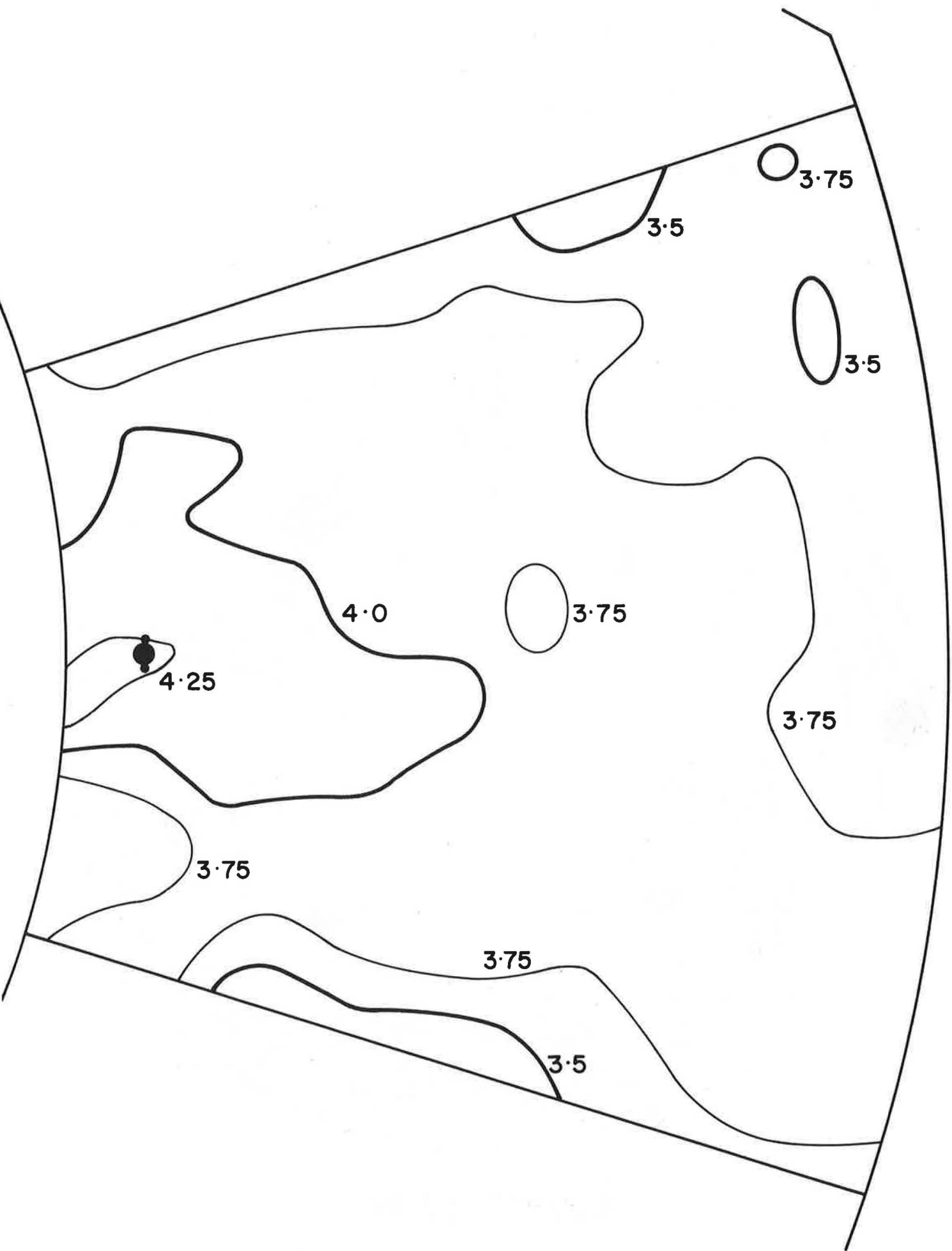


Fig.6    DID4 Contour Map.



